

Original Article

Identification of differentially expressed autophagy genes associated with osteogenic differentiation in human bone marrow mesenchymal stem cells

Yibo Xu^{1,2*}, Zhimeng Wang^{1*}, Yakang Wang^{1*}, Qiang Huang¹, Cheng Ren^{1,2}, Liang Sun¹, Qian Wang¹, Ming Li¹, Hongliang Liu¹, Zhong Li¹, Kun Zhang¹, Teng Ma^{1,2}, Yao Lu^{1,2}

¹Department of Orthopaedic Surgery, Honghui Hospital, Xi'an Jiaotong University, Xi'an 710054, Shaan'xi Province, China; ²Bioinspired Engineering and Biomechanics Center (BEBC), School of Life Science and Technology, Xi'an Jiaotong University, Xi'an 710049, Shaan'xi Province, China. *Equal contributors.

Received February 20, 2022; Accepted July 5, 2022; Epub August 15, 2022; Published August 30, 2022

Abstract: Background: Mesenchymal stem cells derived from human tissues have been widely used for tissue regeneration because of their strong self-renewal capacity and multi-potential properties. Autophagy plays a vital role in maintaining bone homeostasis. However, the mechanism underlying this role for autophagy in the osteogenic differentiation of mesenchymal stem cells remains to be elucidated. Methods: Two microarray datasets were downloaded from the GEO database. Fourteen bone marrow mesenchymal stem cell samples comprising control and induction groups were selected to identify differentially expressed autophagy-related genes via multiple bioinformatics approaches, followed by functional analysis. Interactions among differentially expressed autophagy genes, miRNAs, and transcription factors were analyzed and visualized using Cytoscape software. The association between hub differentially expressed genes and autophagy was validated by qRT-PCR. Results: Ten autophagy-related genes (including *VPS8*, *NDRG4*, and *CYBB*) were identified as osteogenic hub genes. Correlation analysis revealed that *CYBB* was highly correlated with the sensitivity to multiple drugs, such as imexon, megestrol acetate, and isotretinoin. The regulatory network displayed a complex connection among miRNAs, transcription factors, and differentially expressed autophagy genes. Friends' analysis showed that *NDRG4* was highly closely related to other hub genes ($P < 0.05$). Furthermore, *NDRG4* expression was downregulated in the induction group ($P < 0.01$). *NDRG4* was significantly correlated with infiltrating immune cells, including monocytes, eosinophils, type 17 T helper cells, neutrophils, activated CD8 T cells, and immature B cells. Levels of the 10 autophagy-related genes (including *VPS8*, *NDRG4*, and *CYBB*) were successfully validated based on *in vitro* experiments. Conclusion: We identified candidate molecules to further investigate their functions in osteogenesis, providing novel insights into the role of autophagy in mesenchymal stem cell differentiation.

Keywords: Autophagy, differentially expressed genes, mesenchymal stem cells, osteoblast differentiation

Introduction

Bone defects caused by accidental trauma, malignancy resection, or chronic infection remain intractable in clinical settings. The global number of fracture cases was approximately 178 million in 2019, with an incidence of 2,296 cases per 100,000 [1]. The older age group was found to have a higher incidence, particularly in women, compared to the younger age group. The current therapy used for bone reconstruction is surgical grafting, including autografts, allograft tissue, and artificial substi-

tute materials [2, 3]. However, these methods have some limitations. Autografting is hampered by a limited graft supply and complications, leading to an unsatisfactory prognosis [4]. Allografts can trigger acute immunological rejection and viral infection. Moreover, biomaterials do not always fuse well with the host bone and might not always match the functional properties of bone tissues [5]. In recent years, bone tissue engineering has provided a promising clinical choice that utilizes seed cells, scaffold biomaterials, and growth factors to induce vital bone formation [6]. Given their

promising self-renewal capacity and pluripotency, mesenchymal stem cells (MSCs) have been widely used to improve regeneration efficiency [7]. However, little is known about the osteogenic differentiation of MSCs.

Autophagy is a conserved process that maintains intracellular homeostasis by controlling protein degradation and damaged organelle turnover in eukaryotic cells [8]. There are three types of autophagy in mammals, microautophagy, chaperone-mediated autophagy, and macroautophagy, of which macroautophagy is the major autophagic process that contributes to the efficient delivery of cytoplasmic cargo to the lysosome for degradation [9]. Autophagy is a cytoprotective mechanism in cells under stress and is regulated by many pathways. The most extensively studied is the AKT/mammalian target of rapamycin (mTOR) pathway, a main negative regulator of autophagy that functions via the generation of two distinct complexes, mammalian target of rapamycin complex 1 (mTORC1) and mammalian target of rapamycin complex 2 (mTORC2) [10]. The biological activity of MSCs can be affected by the advanced age and comorbidities of donors, which hinder the clinical application of MSCs. Recent evidence has confirmed the fundamental role of autophagy in improving MSC functions in bone formation [11]. For example, long-term exposure to high blood glucose has been implicated in abnormal bone metabolism and impaired bone quality; further, activation of PPAR β/δ can promote osteogenic differentiation of bone marrow MSCs through AMPK/mTOR-mediated autophagy [12]. In aged MSCs, the autophagy level is mostly decreased; however, autophagy activation induced by rapamycin can significantly improve osteogenesis, whereas an autophagy inhibitor was found to reverse this change [13]. Similarly, MSCs from young mice have higher autophagy levels and osteogenic differentiation capacity than those from older mice, and the autophagy inhibitor 3-methyladenine (3-MA) can reduce the osteogenic capacity of MSCs, resulting in an aged state [14]. Thus, the restoration of autophagic activity in MSCs could be explored as a therapeutic strategy for bone defects or fracture healing. Moreover, autophagy participates in the differentiation and function of osteoclasts and osteoblasts during bone formation. Autophagy-

deficient osteoblasts display elevated oxidative stress levels and receptor activator of nuclear factor kappa-B ligand (RANKL) secretion, leading to the generation of osteoclasts and bone resorption [15]. Silencing the autophagy-associated gene *Beclin1* contributes to the inhibition of osteoclast differentiation and maturation [16]. These findings demonstrate a key role for autophagy in osteogenic differentiation and suggest its therapeutic potential for bone healing.

Previous studies have demonstrated the biological changes involved in the osteogenic differentiation of stem cells, such as microtubule and cytoskeleton changes [17]. Here, we focused on the autophagy-mediated osteogenic differentiation of MSCs. Genomic profiles derived from public databases were analyzed to identify differentially expressed genes (DEGs) between control and induced MSCs undergoing osteogenic differentiation. Several autophagy-related genes were screened according to bioinformatics analysis. Further, interactions between MSCs and immune cells are necessary for MSC-mediated immunomodulatory effects during the tissue repair process. Thus, the association between immune cell infiltration and hub genes was investigated. Our results suggest that the identification of autophagy-related genes might provide a better understanding of the osteogenic differentiation of MSCs.

Methods

Data resource and preprocess

Using the GEO query pack [18], two microarray datasets (GSE18043 [19] and GSE12266 [20]) associated with human bone marrow-derived MSCs were downloaded from the public database (<https://www.ncbi.nlm.nih.gov/geo/>). These datasets were tested on the GPL570 [HG-U133_plus_2] Affymetrix Human Genome U133 Plus 2.0 Array. Sample selection was further performed. In the GSE18043 dataset, three normal MSC samples (GSM250019, GSM250020, and GSM250021) and three dexamethasone-treated samples (GSM451159, GSM451160, and GSM451161) were included. In the GSE12266 dataset, four healthy control samples (GSM308067, GSM308071,

Autophagy genes associated with osteogenic differentiation

GSM308075, and GSM308079) and four samples (GSM308070, GSM308074, GSM308078, and GSM308082) induced with mineralization medium containing β -glycerophosphate were selected. These 14 samples were divided into a control group and an induction group for further analysis. Background correction and data normalization were conducted for these datasets, and the combined microarray data with batch effect removal were finally obtained using the SVA package.

Screening differentially expressed autophagy-related genes

The DEGs were screened using the limma package [21]. Volcanic and heat maps were generated using the GGPLOT2 package. $P < 0.05$ and $|\text{fold change (FC)}| > 1.5$ were considered the selection criteria. Through a comparison of autophagy-related genes from GeneCards [22] (<https://www.genecards.org/>), we extracted the overlapping genes as candidate differentially expressed autophagy genes (DEAGs) associated with osteogenesis.

The protein interaction network of DEAGs was analyzed using the STRING database (<https://string-db.org/>) [23]. Cytoscape software and the Cytohubba plugin were used to predict hub DEAGs and visualize their interaction networks. The ClusterProfiler package [24] was applied to conduct functional analysis of Gene Ontology (GO), Kyoto Encyclopedia of Genes (KEGG), and Gene Set Enrichment Analysis (GSEA). The “c2. Cp. Kegg. V7.0. Entrez. GMT” was set as the control set. A false discovery rate < 0.25 and $P < 0.5$ was set as the threshold.

Prediction of miRNAs and transcription factors related to autophagy

For these DEAGs, we predicted correlated miRNAs from the miRtarbase database using the MultiMiR package [25]. Experimental conditions were selected as the “luciferin reporter gene experimental verification”. Transcription factors (TFs) were extracted from the Cistrome [26] database (<http://cistrome.org/db/#/>), and the relationships between TFs and DEAGs were analyzed. The gene pairs that met the criteria of $\text{cor} > 0.9$ and $P < 0.001$ were selected as crucial genes. Cytoscape was used to visualize the interactions.

Relationship between hub gene and drug sensitivity

The PROC package [27] was used to generate receiver operating characteristic (ROC) curves of DEAGs, and the area under the curve (AUC) values of each gene were calculated. Genes with an AUC value greater than 0.9 were selected as hub genes.

The RNA expression dataset and drug data were downloaded from the CellMiner Database (<https://discover.nci.nih.gov/cellminer/>) [28] to investigate the association between hub genes and drug sensitivity. The top 16 terms with significant differences were displayed in the scatter graph using the GGPLOT2 package.

Target gene screening and immune cell infiltration evaluation

The GOSemSim package [29] was employed to conduct Friends' analysis of the hub genes associated with the osteogenic differentiation of MSCs. The differences in target gene expression between the normal group and the treatment group were visualized in the violin diagram using the GGPUBR package. Scatter plots were generated to display the correlation between the target genes and other DEAGs.

Single-sample GSEA analysis [30] was conducted by calculating the rank value of each gene according to the expression profiles. The cellMarker (<http://biocc.hrbmu.edu.cn/CellMarker/>) database [31] is a manually curated resource of cell markers in humans and mice, which contains the markers of 28 types of immune cells. We integrated the gene expression matrix data and Cellmarker data to generate an immune cell infiltration diagram. Heat maps were employed to display the infiltrating status of 28 immune cells in each sample using the pheatmap package (<https://CRAN.R-project.org/package=pheatmap>). A Laplace map was utilized to visualize the correlation between target genes and immune cell infiltration with the Ggplot2 package.

Cell culture and treatment

Mouse MSCs were purchased from Procell Life Science & Technology Co., Ltd. (Wuhan, Hubei, China) and were cultured in complete DMEM

Autophagy genes associated with osteogenic differentiation

Table 1. Primer sequences for qRT-PCR

Gene	Direction	Sequence (5'-3')
LC3-II	Forward	TTATAGAGCGATACAAGGGGGAG
	Reverse	CGCCGTCTGATTATCTTGATGAG
Beclin-1	Forward	ATGGAGGGGTCTAAGGCGTC
	Reverse	TCCTCTCCTGAGTTAGCCTCT
p62	Forward	AGGATGGGGACTTGTTGC
	Reverse	TCACAGATCACATTGGGGTGC
Vps8	Forward	GATGGGGCGTGTCACAAATGC
	Reverse	TCTGAGTTGCCTTCTGCGC
Rbp1	Forward	ATAGACGACCGCAAGTGCAT
	Reverse	CAGATCACACCCTCAGCTCTC
Rps6ka1	Forward	TTCCTGGTACGCAAGGTCAC
	Reverse	ATCTTGGTCCGAACACGGTC
Plat	Forward	TGTGAGCTTTCTGGCTACGG
	Reverse	CAGCATGTTGTTCTGACGG
Ndr4	Forward	CCCAGTGATGCTGGTAGTCG
	Reverse	TCAGCTCCCTGGTTGTGTC
Cybb	Forward	GTTGGTTCGGTTTTGGCG
	Reverse	GATACCTTGGGGCACTTGAC
Rab20	Forward	CGCCTTCTACCTGAAGCAGT
	Reverse	CTGTGGGTGGTTCACATCGT
Mybph	Forward	ACTTAGCCACCACCACCAAG
	Reverse	GTGGAGGTATGGTCAGCCAG
Ceslg	Forward	GGCCATCGCTCAGAGTAGTG
	Reverse	AGCGGAGGTGGTGGTTTTAC
Kih11	Forward	AGTTCGGTGTGGCTGTCATT
	Reverse	GGTGGCAAACAGTCCATGTC

containing 100 U/ml penicillin, 100 µg/ml streptomycin, and fetal bovine serum at 37°C with 5% CO₂. The medium was replaced every 2 days. At passage 3, MSCs were collected for further experiments.

MSCs were divided into two groups, the control group, and the treatment group. MSCs in the treatment group were administered 100 nM rapamycin (MedChemExpress, AY-22989) to induce autophagy. The expression levels of LC3-II, Beclin-1, and p62 were measured to confirm autophagy.

Validation of hub DEGs by qRT-PCR

Total RNA was extracted from cells using TRIzol (Thermo Fisher Scientific, USA) following the manufacturer's instructions and was reverse transcribed into cDNA using the GoScript™ Reverse Transcription System (A5001, Pro-

mega, USA). qRT-PCR was performed using GoTaq® qPCR Master Mix Primers (A6001, Promega, USA) with primers synthesized by GeneCopoeia Inc. (Guangzhou, Guangdong, China). The primers are displayed in **Table 1**. The relative mRNA expression level was analyzed based on the 2^(-ΔΔCT) method.

Statistical analysis

In vitro experiments were repeated three times. Data were expressed as the mean ± standard deviation. Differences between two groups were calculated by performing a t-test using GraphPad Prism software (San Diego, USA). P < 0.05 was regarded as statistically significant.

Results

Identifying DEGs involved in osteogenesis

First, the profiles of GSE18043 and GSE12266 were processed for data normalization (**Figure 1A-D**). The expression matrix of the two datasets was combined with batch effect removal (**Figure 1E, 1F**). We identified a total of 232 DEGs between the induction and control groups, including 145 upregulated and 87 down-regulated genes. The gene distribution and clustering analyses are shown in volcano diagrams and heat maps (**Figure 1G, 1H**).

Screening and functional analysis of DEAGs

We obtained 42 overlapping genes by comparing the DEGs and autophagy-related genes from the GenBank database (**Figure 2A-C**). With the correlation analysis, we finally selected the top 10 genes with significant internal correlations for functional analysis (**Figure 2F**), including *CYBB*, *CCL5*, and *MRC1*. GO analysis showed that DEAGs were mainly associated with the following: extracellular signal-regulated kinase 1 (ERK1)/ERK2 cascade, positive regulation of the ERK1/ERK2 cascade, and regulation of the ERK1/ERK2 cascade; response to molecules of bacterial origin; response to lipopolysaccharide; the DBIRD complex; endocytic vesicles; interleukin-33 binding; and phosphatidylinositol phospholipase C activity (**Figure 3A-D; Table 2**). KEGG analysis revealed enriched pathways associated with these DEGs, including central carbon metabolism in cancer, complement and coagulation cas-

Autophagy genes associated with osteogenic differentiation

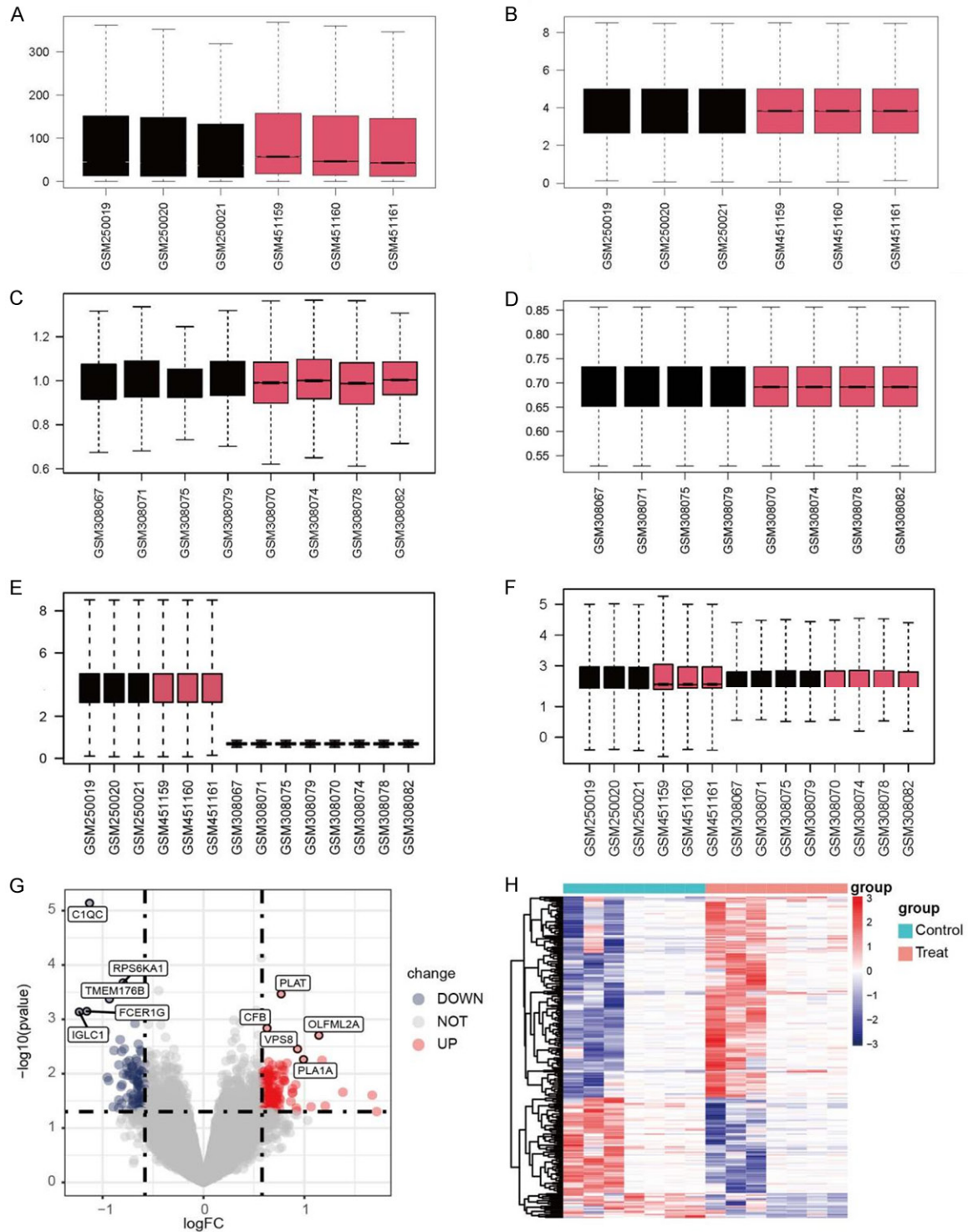


Figure 1. Identification of differentially expressed genes (DEGs) based on the GSE18043 and GSE12266 datasets. (A-F) Boxplots of GSE18043 (A, B), GSE12266, and the combined dataset (E, F) before and after data normalization. (G) Volcano plot of DEGs. Red and blue represent up- and downregulated genes, respectively. (H) Heat maps of the DEGs.

acades, drug metabolism-other species, phago-some, and rheumatoid arthritis (**Figure 3E**; **Table 3**). Additionally, the genes *CYBB*, *MRC1*,

and *NOS1* were found to have important roles in the autophagy-related phagosome pathway (**Figure 3F**). Moreover, GSEA pathways were

Autophagy genes associated with osteogenic differentiation

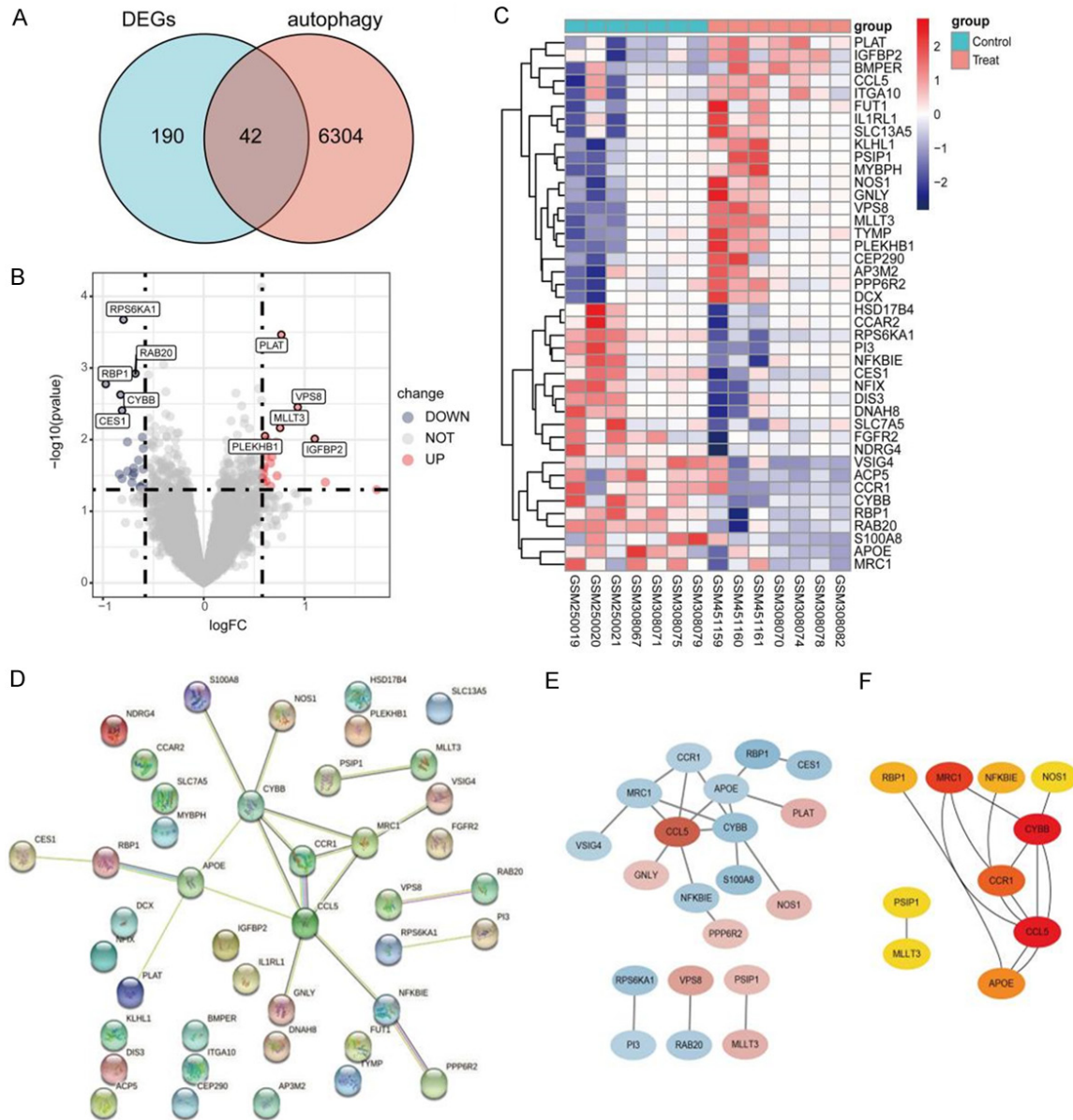


Figure 2. Screening of differentially expressed autophagy genes (DEAGs) related to osteogenesis. A. Venn diagrams of the differentially expressed genes (DEGs) and autophagy genes. B, C. Volcano map and heat map visualization of crucial genes. D, E. Protein-protein interaction network of crucial genes. F. Interaction analysis of the top 10 most important genes derived from the Cytohubba calculation. The darker the color, the closer the gene is to the other molecules.

mainly involved in the autophagy-related mTOR signaling pathway and cytokine-cytokine receptor interaction pathway (**Figure 3G**; **Table 4**).

Identification of target miRNAs and TFs associated with DEAGs

A complex network was generated to visualize the connections among miRNAs, TFs, and DEAGs related to osteogenic differentiation.

In total, 24 miRNAs were obtained from the miRBase database (**Figure 4A**). In the miRNA network, *CCL5* and *SLC7A5* were considered possible hub genes for higher-target miRNA associations. The interactions between the TFs and DEAGs are shown in **Figure 4B**, including 51 connections. Among these DEAGs, *CUX1* and *FOXK1* were identified as the hub genes.

Autophagy genes associated with osteogenic differentiation

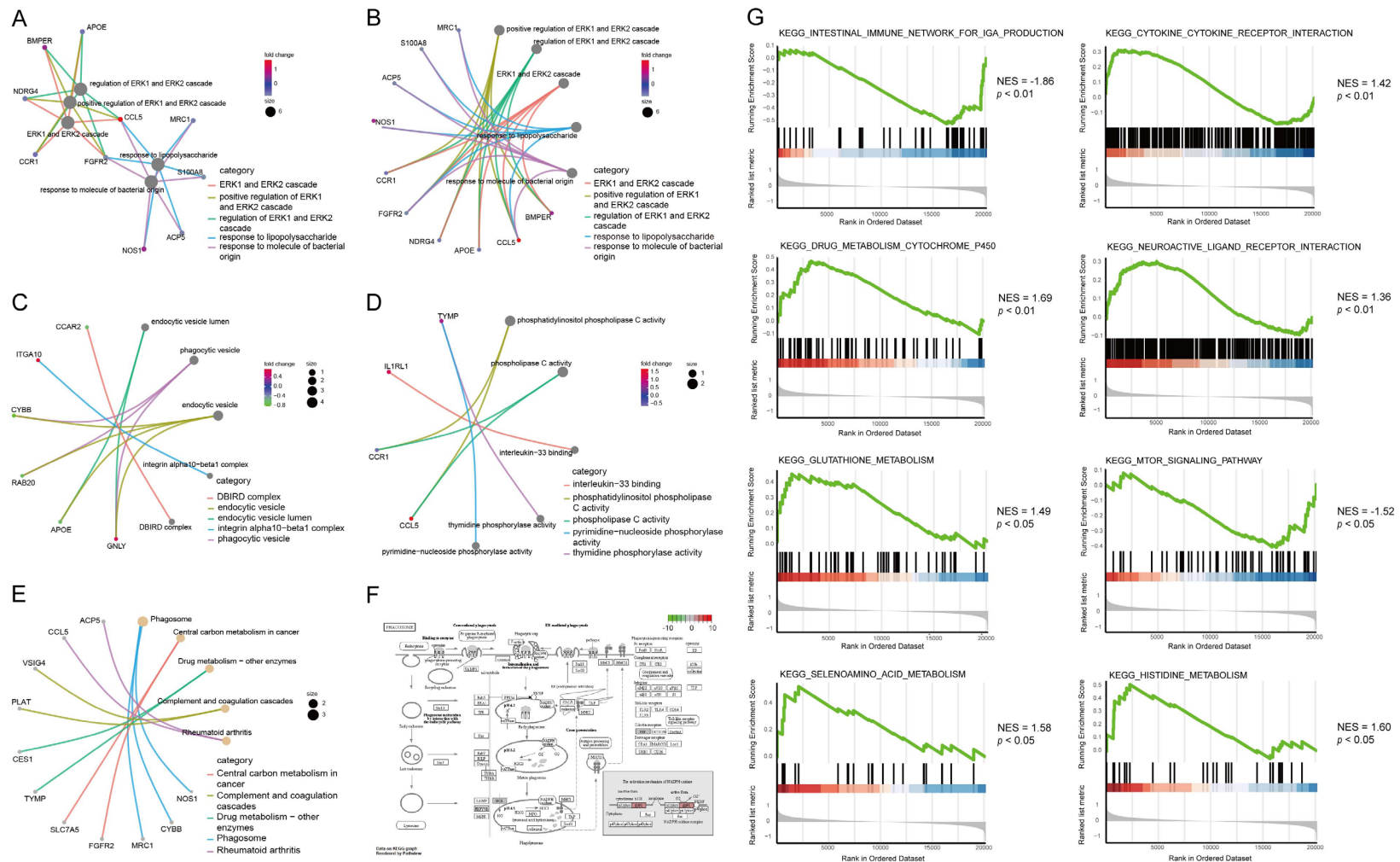


Figure 3. Functional analyses of the differentially expressed autophagy genes (DEAGs). A. Gene ontology (GO) biological function enrichment analysis. The color degree of the point represents the fold-change (FC) value. A darker color indicates a greater FC value. The size of the dot represents the number of enriched genes. B-D. GO terms included biological process (BP), cellular component (CC), and molecular function (MF). E. Kyoto Encyclopedia of Genes and Genomes (KEGG) enrichment analysis. F. Phagosome pathway analysis. G. Gene set enrichment analysis. The P -value was determined based on the Kolmogorov-Smirnov test.

Autophagy genes associated with osteogenic differentiation

Table 2. Gene Ontology (GO) enrichment analysis of differentially expressed autophagy genes (DEAGs)

Ontology	ID	Description	P-value	Q-value
BP	GO:0070374	Positive regulation of ERK1 and ERK2 cascade	8.07E-06	0.009984
BP	GO:0070372	Regulation of ERK1 and ERK2 cascade	5.28E-05	0.027334
BP	GO:0070371	ERK1 and ERK2 cascade	7.16E-05	0.027334
BP	GO:0032496	Response to lipopolysaccharide	8.94E-05	0.027334
BP	GO:0002237	Response to molecule of bacterial origin	0.00011	0.027334
CC	GO:0071682	Endocytic vesicle lumen	0.000821	0.071827
CC	GO:0045335	Phagocytic vesicle	0.002782	0.071827
CC	GO:0030139	Endocytic vesicle	0.003865	0.071827
CC	GO:0034680	Integrin alpha 4-beta1 complex	0.004256	0.071827
CC	GO:0044609	DBIRD complex	0.004256	0.071827
MF	GO:0004435	Phosphatidylinositol phospholipase C activity	0.001488	0.043773
MF	GO:0004629	Phospholipase C activity	0.001725	0.043773
MF	GO:0002113	Interleukin-33 binding	0.002204	0.043773
MF	GO:0009032	Thymidine phosphorylase activity	0.002204	0.043773
MF	GO:0016154	Pyrimidine-nucleoside phosphorylase activity	0.002204	0.043773

BP, biological process; CC, cellular component; MF, molecular function.

Table 3. Kyoto Encyclopedia of Genes and Genomes (KEGG) enrichment analysis of differentially expressed autophagy genes (DEAGs)

ID	Description	P-value	q-value	Count
hsa04145	Phagosome	0.009805	0.374928	3
hsa05230	Central carbon metabolism in cancer	0.017953	0.374928	2
hsa00983	Drug metabolism-other enzymes	0.023074	0.374928	2
hsa04610	Complement and coagulation cascades	0.025836	0.374928	2
hsa05323	Rheumatoid arthritis	0.030519	0.374928	2

Table 4. Pathway enrichment in the Gene Set Enrichment Analysis (GSEA)

ID	setSize	Enrichment	NES	P-value	q-value
KEGG_intestinal immune network for IgA production	44	-0.521390	-1.863520	0.000474	0.084732
KEGG_Cytokine-cytokine receptor interactions	250	0.319194	1.422271	0.002423	0.159993
KEGG_Drug metabolism cytochrome P450	57	0.473399	1.693955	0.002682	0.159993
KEGG_Neuroactive ligand receptor interaction	263	0.302358	1.359049	0.008458	0.378392
KEGG_Glutathione metabolism	47	0.437777	1.494384	0.014437	0.435744
KEGG_mTOR signaling pathway	50	-0.414370	-1.522840	0.016458	0.435744
KEGG_Seleno amino acid metabolism	25	0.527867	1.579686	0.017045	0.435744
KEGG_Histidine metabolism	29	0.510813	1.596933	0.019705	0.440770

NES, Normalized enrichment score.

Hub gene screening and drug sensitivity verification

The AUC value of each gene was calculated, and we selected 10 DEGs as hub genes using the defined criteria (**Figure 5A**), including *VPS8*,

RBP1, *RPS6KA1*, *PLAT*, *NDRG4*, *CYBB*, *RAB20*, *MYBPH*, *CES1*, and *KLHL1*. The functional role of the 10 hub genes is displayed in **Table 5**. Correlation analysis of the hub genes and drug sensitivity revealed that *CYBB* was highly correlated with a variety of drugs such as imexon,

Autophagy genes associated with osteogenic differentiation

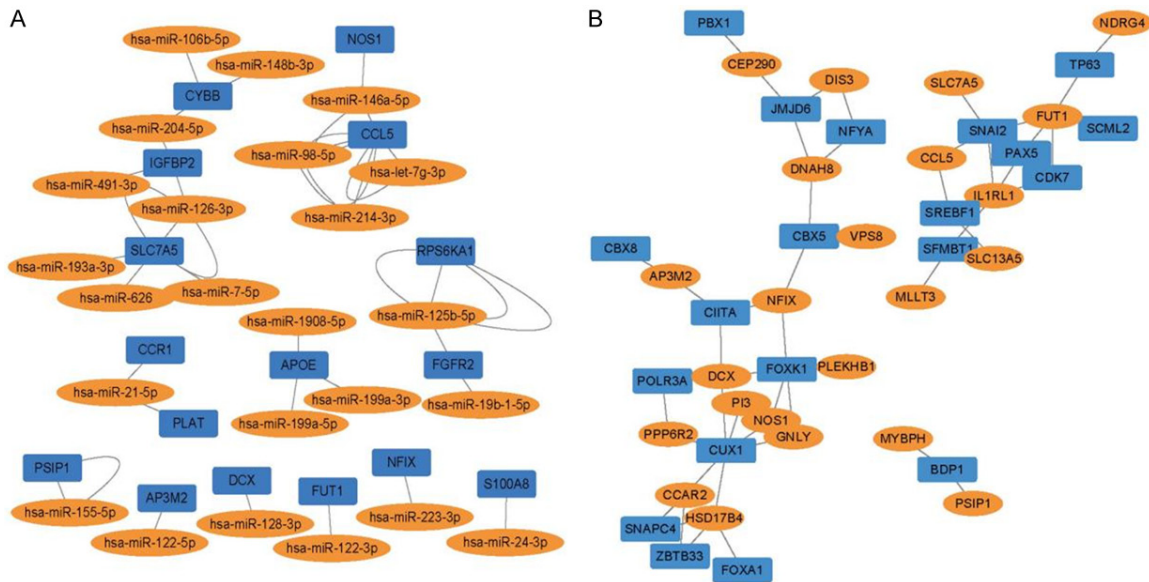


Figure 4. Regulatory network generated to visualize the interactions among miRNA, transcription factors (TFs), and autophagy-related genes. A. Interaction network of the miRNAs and differentially expressed autophagy genes (DEAGs). B. Complex network of the TFs and DEAGs.

megestrol acetate, isotretinoin, denileukin diftitox ontak, nelfinavir, LDK-378, alectinib, dime-thylamino parthenolide, dromostanolone propionate, carmustine, intravenous, and hydroxy-urea (**Figure 5B**).

Target gene screening and immune cell infiltration analysis

Friends' analysis of the hub gene showed that *NDRG4* displayed a high correlation with other genes (**Figure 6A**). The expression of *NDRG4* was positively correlated with *CES1* ($R = 0.73$, $P = 0.0029$), *CYBB* ($R = 0.59$, $P = 0.028$), *RAB20* ($R = 0.59$, $P = 0.027$), and *RPS6KA1* ($R = 0.7$, $P = 0.0056$). However, it was negatively correlated with *PLAT* ($R = -0.6$, $P = 0.023$) and *VPS8* ($R = -0.73$, $P = 0.003$). Furthermore, the expression of *NDRG4* was decreased in the treatment group compared to that in the normal samples (**Figure 6B**, $P < 0.01$).

There was a significant difference in immune cell infiltration between the control and treatment groups (**Figure 7A**). Moreover, the expression of *NDRG4* was correlated with the infiltration of several types of immune cells (**Figure 7B**). Specifically, *NDRG4* was positively correlated with monocytes, eosinophils, gamma delta T cells, central memory CD8 T cells, and T follicular helper cells (**Figure 7C**). Conversely,

five immune cells displayed a negative correlation with *NDRG4*, including CD56dim natural killer cells, type 17 T helper cells, neutrophils, activated CD8 T cells, and immature B cells.

Validation of hub DEGs by qRT-PCR

To validate the association between the 10 selected DEGs, including *VPS8*, *RBP1*, *RPS6KA1*, *PLAT*, *NDRG4*, *CYBB*, *RAB20*, *MYBPH*, *CES1*, and *KLHL1*, and autophagy, we performed validation experiments in MSCs. As shown in **Figure 8A**, the expression levels of *LC3-II*, *Beclin1*, and *p62* were significantly increased after treatment with rapamycin, suggesting that autophagy was successfully induced. The expression levels of *RAB20*, *CES1*, *RBP1*, *KLHL1*, *MYBPH*, *VPS8*, *CYBB*, and *PLAT* were significantly increased ($P < 0.001$), whereas the expression levels of *RPS6KA1* and *NDRG4* were significantly decreased ($P < 0.01$), in the treatment group compared with those in the control group (**Figure 8B**). This result was in accordance with the *in silico* analysis, suggesting the robustness of our analysis.

Discussion

In the present study, we integrated MSC microarray datasets from a public database and screened 232 DEGs between normal and in-

Autophagy genes associated with osteogenic differentiation

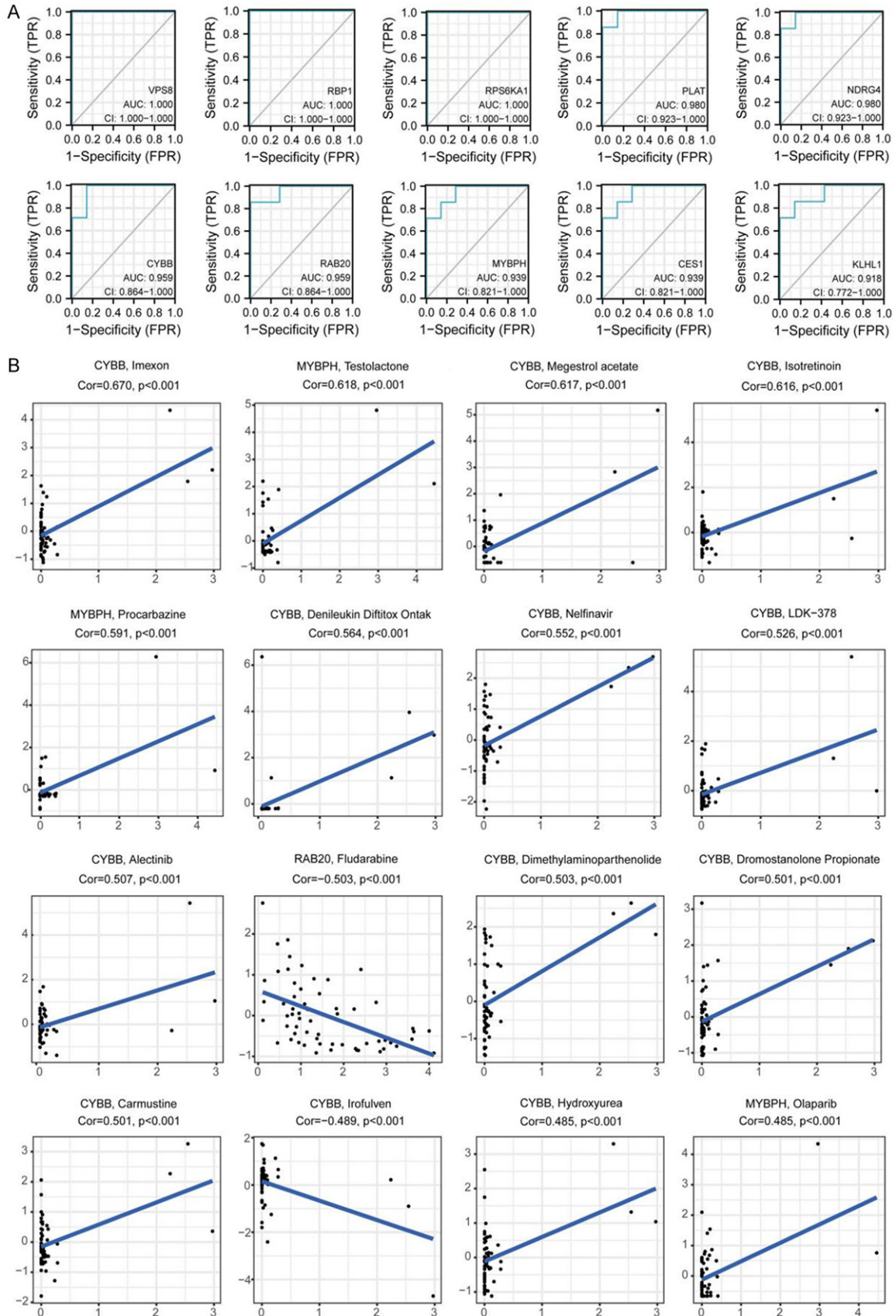


Figure 5. Receiver operating characteristic (ROC) curve (A) and drug sensitivity analysis (B) of the hub genes.

Autophagy genes associated with osteogenic differentiation

Table 5. Functional roles of 10 hub genes

Gene symbol	Full name	Function
<i>VPS8</i>	Vacuolar protein sorting 8 homolog	Protein binding, zinc ion binding
<i>RBP1</i>	Retinol binding protein 1	Intracellular transport of retinol
<i>RPS6KA1</i>	Ribosomal protein S6 kinase	Mediates cellular proliferation, survival, and differentiation by modulating mTOR signaling
<i>PLAT</i>	Plasminogen activator	Plays a direct role in facilitating neuronal migration
<i>NDRG4</i>	NDRG family member 4	Contributes to the maintenance of intracerebral BDNF levels within the normal range
<i>CYBB</i>	Cytochrome b-245, beta polypeptide	Critical component of the membrane-bound oxidase of phagocytes that generates superoxide
<i>RAB20</i>	Member RAS oncogene family	Plays a role in apical endocytosis/recycling
<i>MYBPH</i>	Myosin binding protein H	Binds to myosin
<i>CES1</i>	Carboxylesterase 1	Involved in the detoxification of xenobiotics and in the activation of ester and amide prodrugs
<i>KLHL1</i>	Kelch-like family member 1	Actin binding

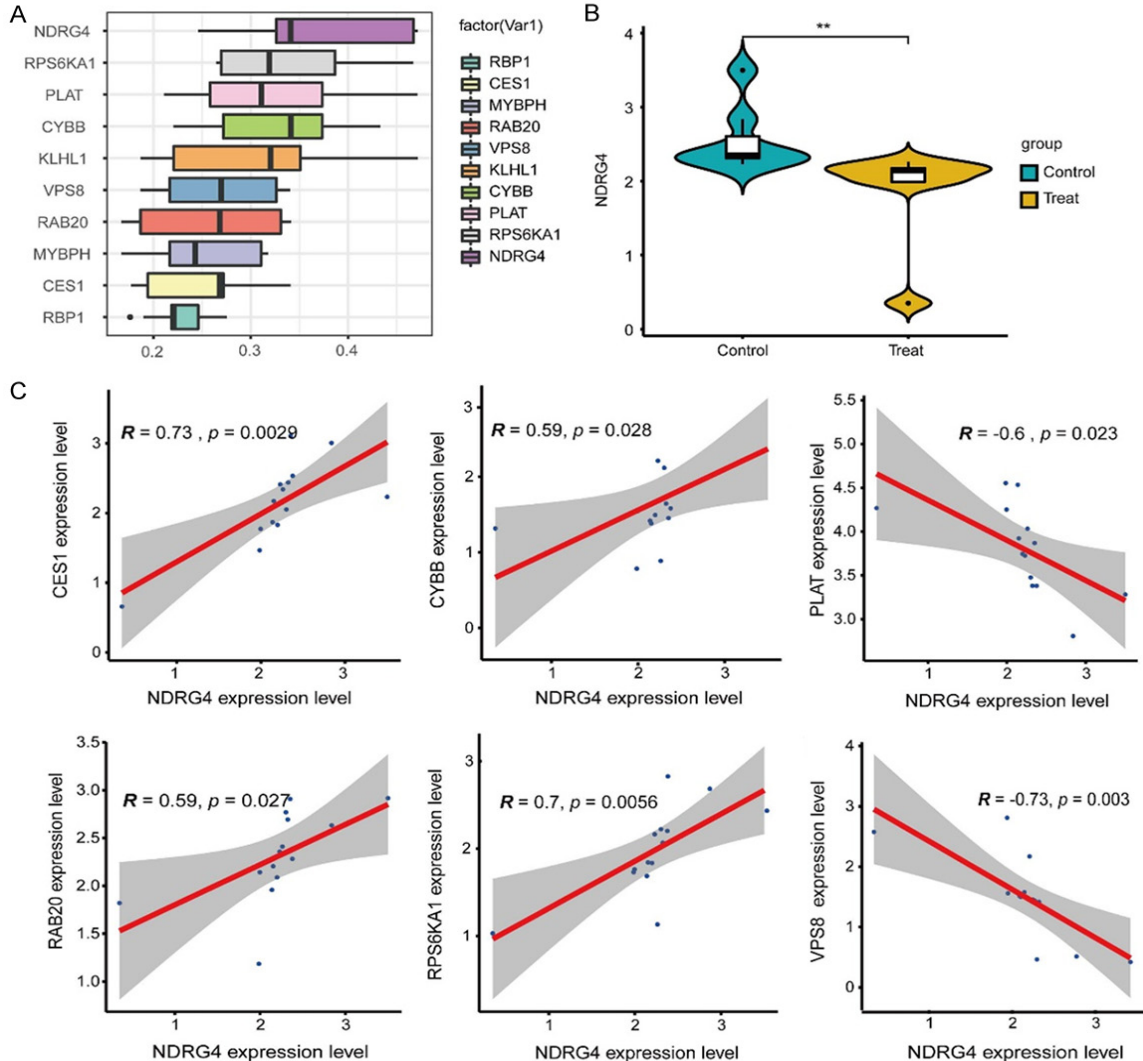
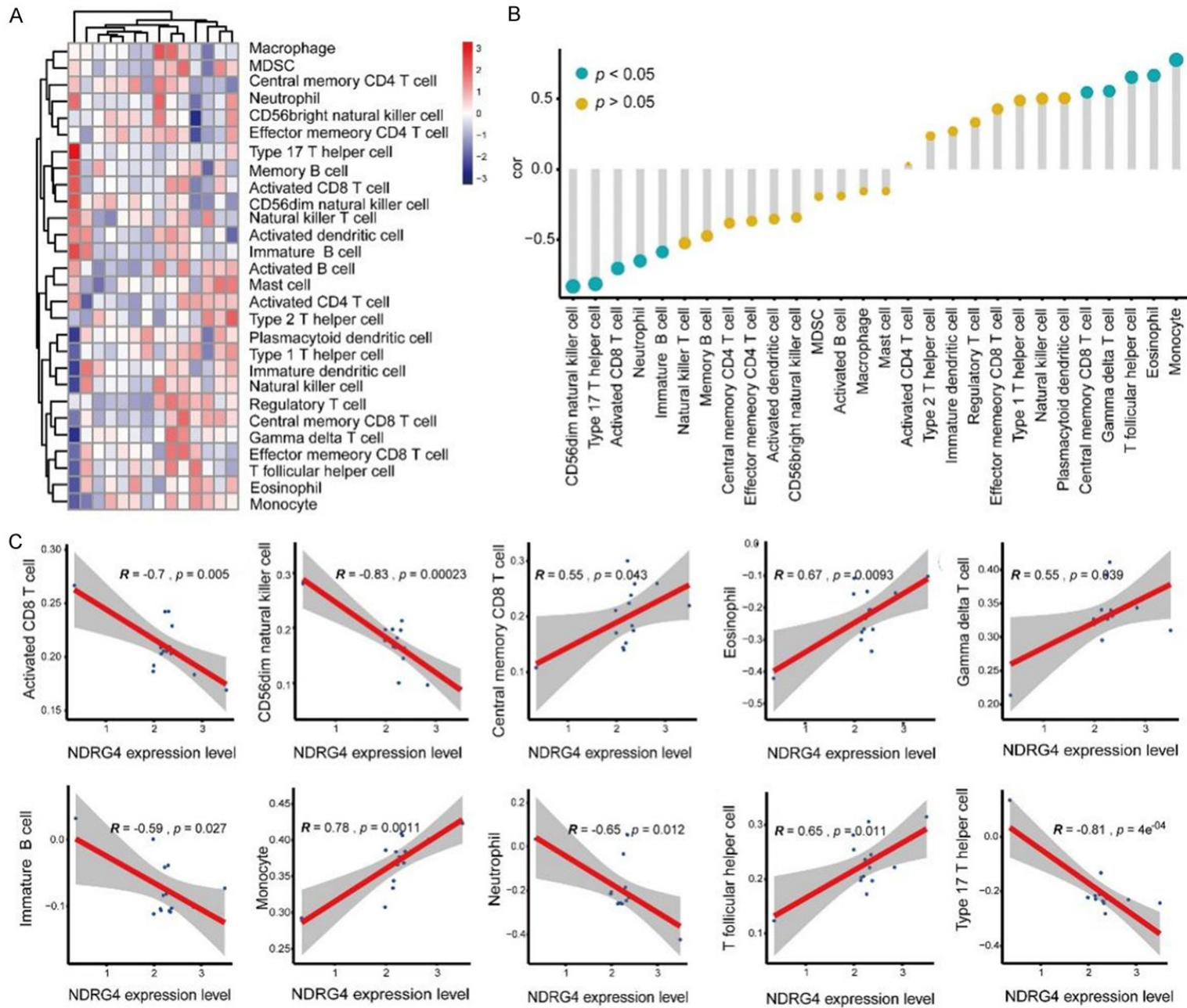


Figure 6. Identification of the hub genes related to the osteogenic differentiation of mesenchymal stem cells (MSCs). A. Friends' analysis of the hub genes related to osteogenesis. B. Expression of *NDRG4* in the different groups. **, $P < 0.01$. C. Correlation analysis of *NDRG4* and other hub genes.

Autophagy genes associated with osteogenic differentiation



Autophagy genes associated with osteogenic differentiation

Figure 7. Correlation analysis of the hub gene and immune cell infiltration. A. Heat map of differences in immune cell infiltration between the control and treatment groups. B. Lollipop diagrams displaying the correlation between *NDRG4* and the infiltration of 28 types of immune cells. Blue and yellow represent $P < 0.05$ and $P > 0.05$, respectively. The larger the dots, the closer the correlation. C. *NDRG4* was correlated with 10 types of immune cells.

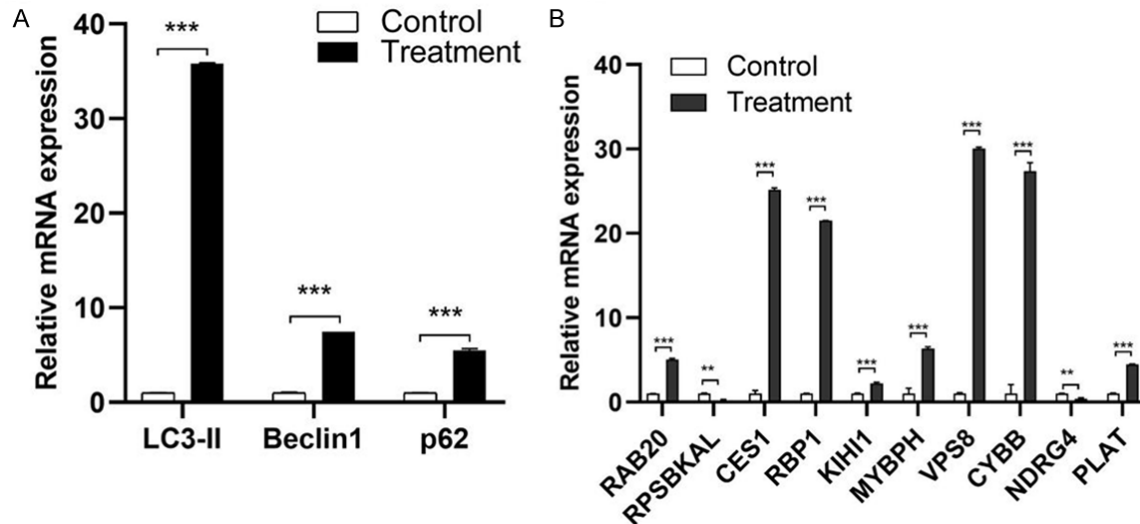


Figure 8. Validation of hub differentially expressed genes (DEGs) by qRT-PCR. A. Relative expression levels of autophagy marker genes, including *LC3-II*, *Beclin1*, and *p62*. B. Relative expression levels of the 10 hub DEGs. Differences between groups were compared with a t-test. **, $P < 0.01$; ***, $P < 0.001$.

duction groups. In total, 42 genes were identified as autophagic genes associated with the osteogenic differentiation of MSCs. Functional enrichment analysis showed that the enriched GO terms included regulation of the ERK1/ERK2 cascade, response to molecules of bacterial origin, and response to lipopolysaccharide. The enriched pathways associated with these genes included the mTOR signaling pathway, central carbon metabolism in cancer, drug metabolism-other species, and the cytokine-cytokine receptor interaction pathway.

Abundant evidence has confirmed that MSC differentiation is a complex and dynamic process governed by a series of chemokines, transcriptional factors, miRNAs, and related signaling pathways. Our study demonstrated the link between DEAGs, corresponding miRNAs, and TFs in this regulatory network. Notably, *CCL5* and *SLC7A5* were highly connected with other miRNAs in the miRNA-DEAG network. The expression of *CCL5* was found to be upregulated during the osteogenic differentiation of MSCs, and the knockdown of endogenous *CCL5* resulted in the suppression of osteogenesis [32]. *SLC7A5* and *LAT1* inhibit osteoclast generation

and function to maintain bone homeostasis via the mTORC1 pathway [33]. According to co-expression network analysis, a recent study reported that *SLC7A5* is associated with the adipogenic and osteogenic differentiation of MSCs [34]. Moreover, *CUX1* and *FUT1* were identified as core factors in the TF-DEAG network. *CUX1* has been reported as a tumor suppressor involved in various types of myeloid neoplasms [35]. *FUT1* could be targeted by *miR-140-5p*, which affects chondrocyte proliferation and autophagy in osteoarthritis [36]. Taken together, these DEAGs, corresponding miRNAs, and TFs might be candidate biomarkers involved in osteogenesis, and further studies are needed to verify their potential functions in MSC differentiation.

Bioinformatics analysis demonstrated that 10 DEAGs, including *VPS8*, *RBP1*, *RPS6KA1*, *PLAT*, *NDRG4*, and *CYBB*, were differentially expressed in bone marrow MSCs undergoing osteogenic differentiation. *CYBB* or *NOX2* encodes the enzyme cytochrome b subunit beta, a major regulator of reactive oxygen species (ROS) generation [37]. The enzyme nicotinamide adenine dinucleotide phosphate (NADPH) oxidase

2 (NOX2) is a multi-subunit complex that consists of membrane-bound subunits and cytosolic components that are separated into resting cells. Upon extracellular stimulation, cytochrome *c* is trafficked to the membrane-bound subunits, forming an active NADPH oxidase complex that promotes ROS generation [38]. An increasing age and higher ROS levels promote MSC differentiation to adipocytes, whereas lower levels of ROS induce osteogenic differentiation [39]. Accordingly, increased intracellular ROS levels in elderly donor-derived MSCs result in reduced osteogenic differentiation potential [40]. ROS affect the transcriptional processes involved in MSC differentiation by interacting with Wnt, Hedgehog, and FOXO signaling pathways [41]. A recent study showed that NOX2 is important for obesity-induced bone remodeling and functions by enhancing bone marrow adiposity and osteoclast generation [42]. Furthermore, our results revealed that *CYBB* is significantly correlated with sensitivity to several drugs, including hydroxyurea. Chemotherapy frequently results in the reduced proliferation of MSCs and decreases osteogenic and adipogenic differentiation [43]. For example, the anticancer agent hydroxyurea could induce bone marrow MSC senescence and decrease osteogenic ability [44]. Therefore, we speculate that *CYBB* might be a major regulator of drug-induced MSC differentiation.

In addition, *NDRG4* exhibited a marked correlation with other genes, according to Friends' analysis. Here, we selected *NDRG4* as a hub gene to explore its regulatory role in osteogenic induction. The expression level of *NDRG4* was decreased in the induced group. *NDRG4* is a member of the *NDRG* family and is mainly expressed in the brain and heart [45]. Further, its deregulation is an important contributor to malignant progression. It has also been reported to be a potential tumor suppressor that is epigenetically inactivated by promoter methylation in colorectal cancer [46]. However, little is known about the role of *NDRG4* in osteogenesis. The abnormal expression of *NDRG4* was correlated with the proportion of certain immune cells, such as activated CD8 T cells, immature B cells, and type 17 T helper cells. Previous studies have confirmed that the immune response is important for the active bone

regeneration program. Proinflammatory T-helper17 cells and secreted cytokines such as interleukin (IL)-17 stimulate the osteoblast differentiation of MSCs [47]. In particular, MSCs exhibit increased osteogenic differentiation ability when exposed to either IL-17A or IL-17F [48]. Additionally, low levels of inflammatory macrophages can induce the autophagic activation of MSCs and promote osteogenic differentiation [49]. These findings indicate that the autophagy-related gene *NDRG4* might be a candidate biomarker involved in MSC osteogenic differentiation and the immune response to bone remodeling. However, the detailed mechanisms need to be elucidated.

There were some limitations to our study. First, the difference in the induction strategy could result in different genomic aberrations in MSCs undergoing osteogenic differentiation. Thus, more samples derived from various databases should be included to verify the accuracy of our results. Second, the effects of these hub genes were all based on bioinformatics analysis, and further experimental studies will be performed in the future.

Overall, our study identified 10 hub genes (*CYBB*, *NDRG4*, *RBP1*, and others) that could be potential biomarkers involved in the osteogenic differentiation of MSCs. A regulatory network was further established to predict the complex interactions among DEAGs, miRNAs, and TFs in osteogenesis. These results provide a novel basis to understand the modulatory role of autophagy in MSC differentiation and bone formation.

Acknowledgements

This work was supported by a project grant from the Scientific Research Program Funded by the Xi'an Health Commission (2021yb26) and Xi'an Science and Technology Project (2019114613YX001SF038(14)).

Disclosure of conflict of interest

None.

Abbreviations

DEAGs, differentially expressed autophagy genes; DEGs, differentially expressed genes;

Autophagy genes associated with osteogenic differentiation

GO, Gene Ontology; GSEA, Gene Set Enrichment Analysis; KEGG, Kyoto Encyclopedia of Genes and Genomes; MSCs, mesenchymal stem cells.

Address correspondence to: Yao Lu and Teng Ma, Department of Orthopaedic Surgery, Honghui Hospital, Xi'an Jiaotong University, 555 Youyi East Road, Xi'an 710054, Shaan'xi Province, China. Tel: +86-029-87800002; E-mail: drluyao@163.com (YL); gukemt@163.com (TM)

References

- [1] Collaborators GF. Global, regional, and national burden of bone fractures in 204 countries and territories, 1990-2019: a systematic analysis from the Global Burden of Disease Study 2019. *Lancet Healthy Longev* 2021; 2: e580-e592.
- [2] Aghali A. Craniofacial bone tissue engineering: current approaches and potential therapy. *Cells* 2021; 10: 2993.
- [3] Wang W and Yeung KWK. Bone grafts and biomaterials substitutes for bone defect repair: a review. *Bioact Mater* 2017; 2: 224-247.
- [4] Lee DJ, Lee YT, Zou R, Daniel R and Ko CC. Polydopamine-laced biomimetic material stimulation of bone marrow derived mesenchymal stem cells to promote osteogenic effects. *Sci Rep* 2017; 7: 12984.
- [5] Bahraminasab M. Challenges on optimization of 3D-printed bone scaffolds. *Biomed Eng Online* 2020; 19: 69.
- [6] Baptista LS, Kronemberger GS, Côrtes I, Charelli LE, Matsui RAM, Palhares TN, Sohier J, Rossi AM and Granjeiro JM. Adult stem cells spheroids to optimize cell colonization in scaffolds for cartilage and bone tissue engineering. *Int J Mol Sci* 2018; 19: 1285.
- [7] Noronha NC, Mizukami A, Caliári-Oliveira C, Cominal JG, Rocha JLM, Covas DT, Swiech K and Malmegrim KCR. Priming approaches to improve the efficacy of mesenchymal stromal cell-based therapies. *Stem Cell Res Ther* 2019; 10: 019-1224.
- [8] Mizushima N and Komatsu M. Autophagy: renovation of cells and tissues. *Cell* 2011; 147: 728-741.
- [9] Wirawan E, Vanden Berghe T, Lippens S, Agostinis P and Vandenabeele P. Autophagy: for better or for worse. *Cell Res* 2012; 22: 43-61.
- [10] Jung CH, Ro SH, Cao J, Otto NM and Kim DH. mTOR regulation of autophagy. *FEBS Lett* 2010; 584: 1287-1295.
- [11] Chen XD, Tan JL, Feng Y, Huang LJ, Zhang M and Cheng B. Autophagy in fate determination of mesenchymal stem cells and bone remodeling. *World J Stem Cells* 2020; 12: 776-786.
- [12] Chen M, Jing D, Ye R, Yi J and Zhao Z. PPAR β / δ accelerates bone regeneration in diabetic mellitus by enhancing AMPK/mTOR pathway-mediated autophagy. *Stem Cell Res Ther* 2021; 12: 566.
- [13] Wan Y, Zhuo N, Li Y, Zhao W and Jiang D. Autophagy promotes osteogenic differentiation of human bone marrow mesenchymal stem cell derived from osteoporotic vertebrae. *Biochem Biophys Res Commun* 2017; 488: 46-52.
- [14] Ma Y, Qi M, An Y, Zhang L, Yang R, Doro DH, Liu W and Jin Y. Autophagy controls mesenchymal stem cell properties and senescence during bone aging. *Aging Cell* 2018; 17: 6.
- [15] Nollet M, Santucci-Darmanin S, Breuil V, Al-Sahlane R, Cros C, Topi M, Momier D, Samson M, Pagnotta S, Cailleteau L, Battaglia S, Farlay D, Dacquin R, Barois N, Jurdic P, Boivin G, Heymann D, Lafont F, Lu SS, Dempster DW, Carle GF and Pierrefite-Carle V. Autophagy in osteoblasts is involved in mineralization and bone homeostasis. *Autophagy* 2014; 10: 1965-1977.
- [16] Guo J, Ren R, Sun K, Yao X, Lin J, Wang G, Guo Z, Xu T and Guo F. PERK controls bone homeostasis through the regulation of osteoclast differentiation and function. *Cell Death Dis* 2020; 11: 847.
- [17] Fan T, Qu R, Yu Q, Sun B, Jiang X, Yang Y, Huang X, Zhou Z, Ouyang J, Zhong S and Dai J. Bioinformatics analysis of the biological changes involved in the osteogenic differentiation of human mesenchymal stem cells. *J Cell Mol Med* 2020; 24: 7968-7978.
- [18] Davis S and Meltzer PS. GEOquery: a bridge between the Gene Expression Omnibus (GEO) and BioConductor. *Bioinformatics* 2007; 23: 1846-1847.
- [19] Hamidouche Z, Fromigué O, Ringe J, Häupl T, Vaudin P, Pagès JC, Srouji S, Livne E and Marie PJ. Priming integrin alpha5 promotes human mesenchymal stromal cell osteoblast differentiation and osteogenesis. *Proc Natl Acad Sci U S A* 2009; 106: 18587-18591.
- [20] Granchi D, Ochoa G, Leonardi E, Devescovi V, Baglio SR, Osaba L, Baldini N and Ciapetti G. Gene expression patterns related to osteogenic differentiation of bone marrow-derived mesenchymal stem cells during ex vivo expansion. *Tissue Eng Part C Methods* 2010; 16: 511-524.
- [21] Ritchie ME, Phipson B, Wu D, Hu Y, Law CW, Shi W and Smyth GK. limma powers differential expression analyses for RNA-sequencing and microarray studies. *Nucleic Acids Res* 2015; 43: 20.
- [22] Stelzer G, Rosen N, Plaschkes I, Zimmerman S, Twik M, Fishilevich S, Stein TI, Nudel R, Lie-

Autophagy genes associated with osteogenic differentiation

- der I, Mazor Y, Kaplan S, Dahary D, Warshawsky D, Guan-Golan Y, Kohn A, Rappaport N, Safran M and Lancet D. The genecards suite: from gene data mining to disease genome sequence analyses. *Curr Protoc Bioinformatics* 2016; 54: 1-1.
- [23] Szklarczyk D, Morris JH, Cook H, Kuhn M, Wyder S, Simonovic M, Santos A, Doncheva NT, Roth A, Bork P, Jensen LJ and von Mering C. The STRING database in 2017: quality-controlled protein-protein association networks, made broadly accessible. *Nucleic Acids Res* 2017; 45: D362-D368.
- [24] Yu G, Wang LG, Han Y and He QY. clusterProfiler: an R package for comparing biological themes among gene clusters. *OmicS* 2012; 16: 284-287.
- [25] Ru Y, Kechris KJ, Tabakoff B, Hoffman P, Radcliffe RA, Bowler R, Mahaffey S, Rossi S, Calin GA, Bemis L and Theodorescu D. The multiMiR R package and database: integration of microRNA-target interactions along with their disease and drug associations. *Nucleic Acids Res* 2014; 42: 24.
- [26] Zheng R, Wan C, Mei S, Qin Q, Wu Q, Sun H, Chen CH, Brown M, Zhang X, Meyer CA and Liu XS. Cistrome data browser: expanded datasets and new tools for gene regulatory analysis. *Nucleic Acids Res* 2019; 47: D729-D735.
- [27] Robin X, Turck N, Hainard A, Tiberti N, Lisacek F, Sanchez JC and Müller M. pROC: an open-source package for R and S+ to analyze and compare ROC curves. *BMC Bioinformatics* 2011; 12: 1471-2105.
- [28] Reinhold WC, Sunshine M, Liu H, Varma S, Kohn KW, Morris J, Doroshow J and Pommier Y. CellMiner: a web-based suite of genomic and pharmacologic tools to explore transcript and drug patterns in the NCI-60 cell line set. *Cancer Res* 2012; 72: 3499-3511.
- [29] Yu G, Li F, Qin Y, Bo X, Wu Y and Wang S. GOSemSim: an R package for measuring semantic similarity among GO terms and gene products. *Bioinformatics* 2010; 26: 976-978.
- [30] Bindea G, Mlecnik B, Tosolini M, Kirilovsky A, Waldner M, Obenauf AC, Angell H, Fredriksen T, Lafontaine L, Berger A, Bruneval P, Fridman WH, Becker C, Pagès F, Speicher MR, Trajanoski Z and Galon J. Spatiotemporal dynamics of intratumoral immune cells reveal the immune landscape in human cancer. *Immunity* 2013; 39: 782-795.
- [31] Zhang X, Lan Y, Xu J, Quan F, Zhao E, Deng C, Luo T, Xu L, Liao G, Yan M, Ping Y, Li F, Shi A, Bai J, Zhao T, Li X and Xiao Y. CellMarker: a manually curated resource of cell markers in human and mouse. *Nucleic Acids Res* 2019; 47: D721-D728.
- [32] Liu YC, Kao YT, Huang WK, Lin KY, Wu SC, Hsu SC, Schuyler SC, Li LY, Leigh Lu F and Lu J. CCL5/RANTES is important for inducing osteogenesis of human mesenchymal stem cells and is regulated by dexamethasone. *Biosci Trends* 2014; 8: 138-143.
- [33] Ozaki K, Yamada T, Horie T, Ishizaki A, Hiraiwa M, Iezaki T, Park G, Fukasawa K, Kamada H, Tokumura K, Motono M, Kaneda K, Ogawa K, Ochi H, Sato S, Kobayashi Y, Shi YB, Taylor PM and Hinoi E. The L-type amino acid transporter LAT1 inhibits osteoclastogenesis and maintains bone homeostasis through the mTORC1 pathway. *Sci Signal* 2019; 12: eaaw3921.
- [34] Liu Y, Tingart M, Lecouturier S, Li J and Eschweiler J. Identification of co-expression network correlated with different periods of adipogenic and osteogenic differentiation of BMSCs by weighted gene co-expression network analysis (WGCNA). *BMC Genomics* 2021; 22: 021-07584.
- [35] Aly M, Ramdzan ZM, Nagata Y, Balasubramanian SK, Hosono N, Makishima H, Visconte V, Kuzmanovic T, Adema V, Nazha A, Przychodzen BP, Kerr CM, Sekeres MA, Abazeed ME, Nepveu A and Maciejewski JP. Distinct clinical and biological implications of CUX1 in myeloid neoplasms. *Blood Adv* 2019; 3: 2164-2178.
- [36] Wang Z, Hu J, Pan Y, Shan Y, Jiang L, Qi X and Jia L. miR-140-5p/miR-149 affects chondrocyte proliferation, apoptosis, and autophagy by targeting FUT1 in osteoarthritis. *Inflammation* 2018; 41: 959-971.
- [37] Panday A, Sahoo MK, Osorio D and Batra S. NADPH oxidases: an overview from structure to innate immunity-associated pathologies. *Cell Mol Immunol* 2015; 12: 5-23.
- [38] Grauers Wiktorin H, Aydin E, Hellstrand K and Martner A. NOX2-derived reactive oxygen species in cancer. *Oxid Med Cell Longev* 2020; 2020: 7095902.
- [39] Atashi F, Modarressi A and Pepper MS. The role of reactive oxygen species in mesenchymal stem cell adipogenic and osteogenic differentiation: a review. *Stem Cells Dev* 2015; 24: 1150-1163.
- [40] Tan J, Xu X, Tong Z, Lin J, Yu Q, Lin Y and Kuang W. Decreased osteogenesis of adult mesenchymal stem cells by reactive oxygen species under cyclic stretch: a possible mechanism of age related osteoporosis. *Bone Res* 2015; 3: 15003.
- [41] Li Q, Gao Z, Chen Y and Guan MX. The role of mitochondria in osteogenic, adipogenic and chondrogenic differentiation of mesenchymal stem cells. *Protein Cell* 2017; 8: 439-445.
- [42] Rahman MM, El Jamali A, Halade GV, Ouhitit A, Abou-Saleh H and Pintus G. Nox2 activity is required in obesity-mediated alteration of bone

Autophagy genes associated with osteogenic differentiation

- remodeling. *Oxid Med Cell Longev* 2018; 2018: 6054361.
- [43] Somaiah C, Kumar A, Sharma R, Sharma A, Anand T, Bhattacharyya J, Das D, Deka Talukdar S and Jaganathan BG. Mesenchymal stem cells show functional defect and decreased anti-cancer effect after exposure to chemotherapeutic drugs. *J Biomed Sci* 2018; 25: 5.
- [44] Kapor S, Vukotić M, Subotički T, Đikić D, Mitrović Ajtić O, Radojković M, Čokić VP and Santibanez JF. Hydroxyurea induces bone marrow mesenchymal stromal cells senescence and modifies cell functionality in vitro. *J Pers Med* 2021; 11: 1048.
- [45] Zhou RH, Kokame K, Tsukamoto Y, Yutani C, Kato H and Miyata T. Characterization of the human NDRG gene family: a newly identified member, NDRG4, is specifically expressed in brain and heart. *Genomics* 2001; 73: 86-97.
- [46] Melotte V, Lentjes MH, van den Bosch SM, Hellebregkers DM, de Hoon JP, Wouters KA, Daenen KL, Partouns-Hendriks IE, Stessels F, Louwagie J, Smits KM, Weijenberg MP, Sanduleanu S, Khalid-de Bakker CA, Oort FA, Meijer GA, Jonkers DM, Herman JG, de Bruijne AP and van Engeland M. N-Myc downstream-regulated gene 4 (NDRG4): a candidate tumor suppressor gene and potential biomarker for colorectal cancer. *J Natl Cancer Inst* 2009; 101: 916-927.
- [47] Croes M, Öner FC, van Neerven D, Sabir E, Kruyt MC, Blokhuis TJ, Dhert WJA and Alblas J. Proinflammatory T cells and IL-17 stimulate osteoblast differentiation. *Bone* 2016; 84: 262-270.
- [48] Liao C, Zhang C, Jin L and Yang Y. IL-17 alters the mesenchymal stem cell niche towards osteogenesis in cooperation with osteocytes. *J Cell Physiol* 2020; 235: 4466-4480.
- [49] Yang L, Xiao L, Gao W, Huang X, Wei F, Zhang Q and Xiao Y. Macrophages at Low-Inflammatory Status Improved Osteogenesis via Autophagy Regulation. *Tissue Eng Part A* 2021; [Epub ahead of print].